PERGAMON

Deep-Sea Research II 45 (1998) 2253–2267

DEEP-SEA RESEARCH
PART II

Variability in primary production as observed from moored sensors in the central Arabian Sea in 1995

J. Marra[a,*], T.D. Dickey[b], C. Ho[a], C.S. Kinkade[a], D.E. Sigurdson[b], R.A. Weller[c], R.T. Barber[d]

[a]*Lamont-Doherty Earth Observatory of Columbia University, Palisades, NY 10964, USA*
[b]*ICESS/Department of Geography, UC, Santa Barbara, CA 93106-3060, USA*
[c]*Woods Hole Oceanographic Institution, Woods Hole, MA 02543, USA*
[d]*Marine Laboratory, Duke University, Beaufort, NC, USA*

Received 6 September 1997; received in revised form 5 May 1998; accepted 19 May 1998

Abstract

Carbon assimilation was calculated using surface irradiance and fluorescence data collected from moored sensors located in the Arabian Sea (15°30′N, 61°30′E), beginning the twelve-month period in October 1994. The calculation uses an assumed quantum efficiency and independently estimated phytoplankton absorption coefficients. Fluorescence was calibrated to chlorophyll *a*. Estimated primary production (C assimilation) varied seasonally and was roughly correlated with chlorophyll *a* biomass. Variations in integral primary production estimated from the moored observations as a function of integral chlorophyll *a* are interpreted in terms of the variations in mixed layer depth and possible losses of chlorophyll *a* biomass. Deep mixed layers suggest lower chlorophyll *a*-specific production, and variations in chlorophyll *a* may indicate grazing losses. Seasonal variability in a measure of primary production is useful for establishing the relationship with environmental forcing in the Arabian Sea and in understanding the export of production to the deep sea.

1. Introduction

Biological observations from moored sensors are increasingly used to examine ocean variability not accessible from ships. Although the observations are often

*Corresponding author. Fax: 001 914 365 8150; e-mail: marra@ldeo.columbia.edu

0967-0645/98/$–see front matter
PII: S0967-0645(98)00070-8

limited to a single geographic location, they have proved effective in providing a seasonal context for less frequent shipboard programs (Dickey et al., 1993) and also for examining variability at the diel time scale (e.g., Stramska and Dickey, 1992; Marra, 1997).

Two common types of measurements in mooring observations have relevance to biological dynamics: the fluorescence of chlorophyll *a*, and photosynthetically active radiation (400–700 nm), E_{PAR}. These two variables are advantageous because they are the basic ingredients of models that can be used to calculate primary production in the sea (Bidigare et al., 1987; Marra et al., 1992; Bidigare et al., 1992; Zaneveld et al., 1993). Moored observations can be used to extend observational programs, not only in terms of the variability in autotrophic biomass, but in the rate of primary production as well. The mooring thus offers the opportunity to provide improved estimates of the annual rate of primary production for a region. The annual rate of primary production is useful in understanding how large-scale ocean processes drive productivity (fertility), how the ocean might change on climatological time-scales, and the dynamics of longer-lived members of the ecosystem, such as fish. However, the annual rate is difficult to estimate. Usually, there are not the resources to undertake the sampling required, that is, to occupy a station, repeatedly to calculate the annual estimate. Moored observations, coupled with a biological model, can be adequate substitutes, and, in the absence of satellite observations, may be the only recourse.

A preliminary overview of the data set from the mooring array deployed in the Arabian Sea from October 1994 to October 1995 is described in Rudnick et al. (1997). The array consisted of four moorings in a square ($\sim$7 km on a side) surrounding a fifth, central, surface mooring. At the SW and NW corners were moorings carrying meteorological sensors, acoustic Doppler current profilers (ADCPs) and temperature sensors. At the two eastern corners, sub-surface moorings were instrumented with profiling current meters (Eriksen et al., 1982), which moved up and down the mooring wire at 4 h intervals, recording water velocities, temperature and salinity. The central mooring carried meteorological sensors, temperature and salinity recorders, bio-optical sensors, and oxygen sensors, and recorded the data that are analyzed here (See Fig. 1 in Smith, 1998). The mooring array was centered at 15°30′N,61°30′E. The first deployment of the mooring was from 15 October 1994, until recovery on 17 April 1995. The second deployment was from 22 April 1995, to 20 October 1995. Dickey et al. (1998) describe other aspects of the data, and Weller et al. (1998) describe the meteorological data from the central mooring. Kinkade et al. (1998) examine the diel variability of the bio-optical sensors. Here we use the chlorophyll *a* fluorescence and surface irradiance data to estimate the seasonal variability in primary production from basic principles, relying only on the data supplied by the moored sensors. There are, of necessity, many assumptions in our analysis and validation data are few. Thus, we focus on the variability in primary production rather than its absolute accuracy. Nevertheless, we can study how production responds to the monsoons, and also look at how variability in the surface layer correlates with estimates of the export flux of fixed carbon.

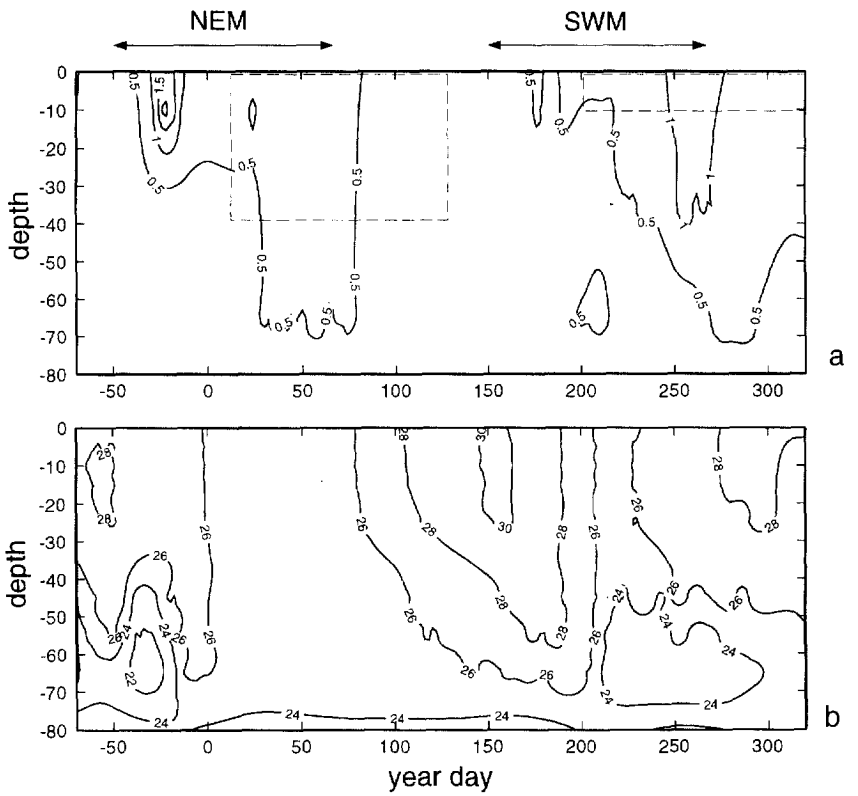

Fig. 1. (a) A time-depth map of chlorophyll *a* (mg m^{-3}) distributions determined from the moored sensors. The sensors were located at 10, 35, 65, and 80 m. The dashed-line boxes enclose times and depths where the sensors became fouled, and therefore those data were discarded. Data from shipboard profiles for when the ship visited the mooring location were used to fill in the time series during these periods. The remainder of the data were interpolated using the gridding scheme in Generic Mapping Tools (GMT, see text). The arrows above the figure denote the period of the northeast (NEM) and southwest (SWM) Monsoons. (b) Temperature (°C) vs time and depth (m) in the upper water column. This plot was assembled from temperature pods located at several depths in the upper water column and from the thermistors on the MVMS' and VMCM's (see Weller et al., 1998). The contours were mapped by GMT.

2. Methods

2.1. General

The technology and procedures follow previously published work on bio-optical variability observed from moorings (Dickey et al., 1991; Marra et al., 1992). The details regarding deployment, sensor performance, calibrations, validation, and data reduction can be found in a series of data reports (Trask et al., 1995a, b; Ho et al., 1996a, b; Sigurdson et al., 1995, 1996; Baumgartner et al., 1997). The primary variables

used in this analysis were from in vivo fluorescence (Fluorometer, SeaTech, Corvallis, OR), and the short-wave radiation sensor of an Improved Meteorological (IMET) system (Precision Spectral Pyranometer, Eppley Instr.) on the surface buoy. A schematic of the mooring is shown in Fig. 2 of Dickey et al. (1998). The fluorometers and PAR sensors were attached to the mooring as part of multi-variable moored systems (MVMS') at 10, 35, 65, and 80 m.

Because of the necessity for long deployments ($\sim$6 mos) in this high-temperature and high-light environment, fouling adversely affected the sensors, particularly the bio-optical sensors. Therefore, we do not have complete records for some of the instruments. As a result, shipboard data collected at the mooring site were used where possible, to fill in data to provide as complete a picture as possible of the time and depth distribution of chlorophyll *a*. All chlorophyll *a* data were gridded using the contouring routine in Generic Mapping Tools (Wessel and Smith, 1992), producing Fig. 1. The times at which the fluorometers became fouled were relatively easy to identify since the voltage from the sensor increased exponentially to its upper limit (5 V) and remained at that value (see Ho et al., 1996a, b).

The times at which the E_{PAR} sensors fouled were less easy to identify because for them it is not an "either-or" situation. There is no optical window, and the teflon collectors do not promote microbial growth, so fouling proceeds much more slowly. Because of the tentative determination of fouling on the E_{PAR} sensors, we instead relied on the short-wave sensor of the meteorological buoy (Weller et al., 1998), calculating E_{PAR} as,

$$E_{PAR}(0) = SW f_1 f_2 \tag{1}$$

where SW is the short-wave radiation value, f_1 converts $W m^{-2}$ to mol photon $m^{-2} s^{-1}$, and has the value 4.15, and f_2 is the fraction of short-wave radiation (300–3000 nm) that is PAR (400–700 nm), and is 0.50, according to Baker and Frouin (1987) the value expected for tropical atmospheres. $E_{PAR}(0^+)$ was converted to $E_{PAR}(0^-)$ using the relationship derived in Siegel and Dickey (1987).

2.2. The calculation of carbon assimilation

Carbon assimilation from the moored sensor data was calculated from

$$P(z) = a^*_{ps} Chl(z) \Phi(z) E_{PAR}(z) \tag{2}$$

where $P(z)$ is the carbon assimilation at depth z, a^*_{ps} is the integrated and averaged chlorophyll *a*-specific absorption coefficient for phytoplankton (corrected for non-photosynthetic pigment; see below), Φ is the quantum yield for carbon fixation, and E_{PAR} is the irradiance from Eq. (1). We have not included a wavelength dependence in the production equation, primarily because the sensors do not provide that information. Other limitations are discussed later. Irradiance at depth, z, is

$$E_{PAR}(z) = E_{PAR}(0^-) e^{-k_{tot} z} \tag{3}$$

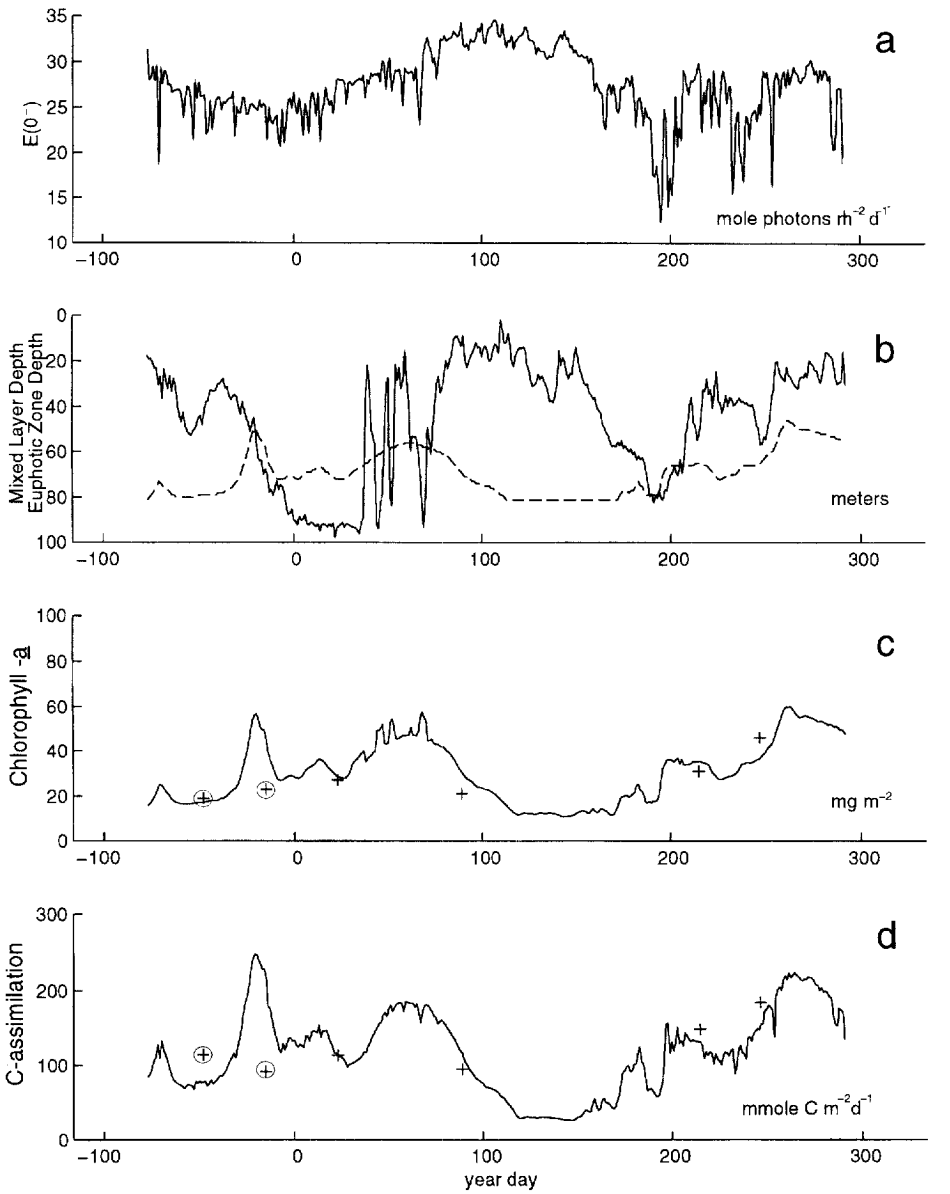

Fig. 2. (a) Surface irradiance, (b) mixed layer and euphotic zone (1% of surface irradiance) depths, (c) areal chlorophyll *a*, (d) areal carbon assimilation. In (c) and in (d), also are plotted the areal chlorophyll *a* and in situ carbon assimilation values from six cruises from Station S07 (16°N/62°E; nearest the mooring). TN053 and TN054 occurred after the mooring was recovered, but these are plotted for additional comparisons (circled symbols) one year early.

where k_{tot} is the total diffuse attenuation coefficient. It is the sum of the sources of attenuation, or

$$k_{tot} = k_w + k_x + a^*_{ph} Chl(z)(1/\bar{\mu}) \tag{4}$$

The attenuation of pure water, k_w, is assigned the value 0.03 m^{-1}, as a reasonable approximation of pure water attenuation irrespective of wavelength (Wozniak et al., 1992). The attenuation of "other" properties, k_x, is not well known. Gelbstoff absorption is small (Coble et al., 1997), however its value can set the magnitude of primary production since it is as large as the other two terms, although potentially not as variable. Here, we assign the value of 0.02 m^{-1} following the data found in Smith et al. (1987).

The last term in Eq. (2) is the phytoplankton absorption coefficient, averaged over the wavelength range of 400–700 nm, and normalized to chlorophyll *a*. To be considered in relation to other sources of attenuation, the absorption coefficient has to be corrected for the average cosine, $\bar{\mu}$, which specifies the angular distribution of the submarine light field. A reasonable value for $\bar{\mu}$ is 0.8 (e.g., Kirk, 1994) and we adopt that value here.

We arrive at a value a^*_{ph} as follows. We begin by using the method in Wozniak et al. (1992), which consists of summing absorption contributions in the red, green, and blue regions of the spectrum. The primary variable affecting a^*_{ph} in this scheme is the pigment index, here designated BR, and which is essentially the ratio of blue to red absorption. *BR* is an empirical function of the trophic state of the region, defined by a range of chlorophyll *a* values, and inversely proportional. For "intermediate" waters, the value for *BR* can be assumed to be 3.7. The equation (Wozniak et al., 1992) used to calculate $a^*_{ph}(\lambda)$ is

$$a^*_{ps}(\lambda) = 0.0187\mathrm{BR}\exp(-0.00012(\lambda-441)^2) + 0.00645\exp(0.00035)(\lambda-608)^2) + 0.0133\exp(-0.00014(\lambda-675)^2). \tag{5}$$

We also assume that the photosynthetic portion of $a^*_{ph}(\lambda)$ is a constant fraction,

$$a^*_{ps}(\lambda) = nps\, a^*_{ph}(\lambda) \tag{6}$$

where *nps* in the above equation represents the fraction of non-photosynthetic pigment absorption, and we assign its value at 0.4. The averaged value for $a^*_{ps}(\lambda)$ was found by

$$\bar{a}^*_{ps} = \frac{\int_{400}^{700} a^*_{ps}(\lambda)\mathrm{d}\lambda}{700-400} \tag{7}$$

and has the value 0.0157 m^{-2} $(mg\,chl)^{-1}$. A similar integration was done for $a^*_{ph}(\lambda)$ for use in the phytoplankton attenuation term in Eq. (4).

Finally, we assume that quantum yield is proportional to irradiance using the equation presented in Bidigare et al. (1992),

$$\Phi(z) = \Phi_{max} \tanh\left(\frac{K\phi}{E_{PAR}(z)}\right) \tag{8}$$

where Φ_{max} is set at 0.06 mol C(mol photons)$^{-1}$, and K_ϕ is a constant with a value of 10 mol photon m^{-2} d^{-1}. These constants have been used in other studies of this type (Kiefer and Mitchell, 1983; Marra et al., 1992).

To avoid possible artifacts associated with non-photochemical quenching of fluorescence, chlorophyll *a* values are from the early morning of each 24 h period, and irradiance is the daily integral. For presentation here, chlorophyll *a* and carbon assimilation were integrated over the euphotic zone. However, for chlorophyll *a*, we made the further assumption that when the mixed layer was deeper than the euphotic zone, the mixed populations still contributed to areal production. However, when the mixed layer depth was shallower than the depth of the euphotic zone, suggesting a stratified water column, only chlorophyll *a* down to the depth of the euphotic zone was used in the calculation of carbon assimilation. Again, the main ingredients to the calculation are the chlorophyll *a* concentration (as a measure of biomass, and as a source of attenuation) and surface irradiance.

It is useful to note that the variables and parameters in Eq. (2) apply to a daily rate of carbon assimilation. For example, $E_{PAR}(0^-)$ is an integral (total, daily) value. Thus, the concerns in arriving at a biassed estimate of integral production because of averaging the irradiance flux coupled with the non-linearities in the photosynthetic response (Platt et al., 1984) do not apply to our analysis.

3. Results

As an indication of the environmental variability observed by the mooring, Fig. 1 shows the variations in temperature in the upper water column. The monsoon periods (see Smith, 1998) are indicated. The seasonal cycle from October 1994, through September 1995, consists of two periods of deeper mixing, associated with the NE and SW monsoons, and two periods of stronger stratification during intermonsoon periods. Convective cooling produces the deep mixed layers during the NE Monsoon, whereas wind-induced stirring deepens the mixed layer during the SW Monsoon (Fischer, 1997; Dickey et al., 1998). The water column structure of chlorophyll *a* (Fig. 1a) shows that it roughly follows the seasonal cycle in the mixed layer depth. Deeper mixed layers are associated with more uniform distributions of chlorophyll *a* over the top 80 m. During the strongest stratification of the year, during May and June, chlorophyll *a* is at a minimum.

We expect that values observed at the mooring were the result of the advection of properties as well as local phenomena. There is evidence of eddy variability in the early parts of each monsoon (see Dickey et al., 1998). Also, one dimensional models, forced by local fluxes, do well at predicting sea-surface temperatures until the middle of the SW monsoon (July–August). At that time there is evidence that cool water is being advected from the Omani coast to the mooring site (current directions at the mooring are ESE). The mixed-layer depth was well predicted using these 1-D models, except during the monsoons, when the passage of the eddies plays a role in setting mixed layer depth (Fischer, 1997).

But the major, seasonal, chlorophyll *a* signals are associated with the re-stratification of the water column near the end of the monsoons. The association of re-stratification with increases in water column chlorophyll *a* is more obvious at the end of the SW Monsoon. At the end of the NE Monsoon, a highly variable mixed layer depth (not observable here, but see Fig. 2) may be responsible for the increase in chlorophyll *a* seen during that period.

Fig. 2 shows surface irradiance, mixed layer depth (change of 0.1°C from sea-surface temperature) and euphotic zone depths (1% of surface irradiance), the calculated areal chlorophyll *a*, and carbon assimilation, all for the entire year. Surface irradiance varies by $\pm$ 5 mol photon $m^{-2} d^{-1}$ over the season, or about 20%, except that increased cloudiness during the SW Monsoon decreases $E_{PAR}(0^-)$ by as much as 80% (see Weller et al., 1998). Variability caused by clouds is apparent during both monsoons, and less so during the spring intermonsoon. The variability in the mixed layer depth shows the effects of each monsoon. The increase in stratification at the cessation of the winds appears to be accompanied by highly variable mixed-layer depths. Calculation of the mixed-layer depth is hindered by the reduced depth resolution inherent with moorings of this type. But current velocities are very low during this period (Rudnick et al., 1997), thus it is unlikely that the variable mixed layer depths result from advective features moving past the mooring (Dickey et al., 1998).

When examined over the year, areal chlorophyll *a* (Fig. 2c) is related to the mixed layer depth, perhaps more clearly shown here than from the contour plots (Fig. 1). Low values coincide with times when the mixed layer is deep (January; days 1–30), or during periods of prolonged stratification (April–June; days 90–200). Higher values occur when the water column re-stratifies near the end of each monsoon period (February–March, July–September). (The variability in areal chlorophyll *a* at this time also occurs because we chose to integrate over the depth of the mixed layer when the mixed layer was deeper than the euphotic zone). Within-season variability in integral chlorophyll *a* is caused by both local and advective phenomena. The peaks in chlorophyll *a* (and shallow mixed layers) during the first few months of the mooring are probably associated with eddies. On the other hand, the increase in chlorophyll *a* during the SW Monsoon follows the shoaling of the mixed layer depth, modified by local changes in insolation (just before day 200). Seasonally, there are two periods of high chlorophyll *a* during the year, both in the latter parts of the monsoons, when the water column begins to re-stratify. The seasonal changes can be obscured by shorter-term variability from advective phenomena, such as eddies.

Productivity, as calculated by Eq. (2), follows the variability in chlorophyll *a*, but only to a certain extent. Thus, chlorophyll *a*-specific production varies over the course of the year. The early data show an apparent direct relationship; however, the chlorophyll *a* maximum in February and early March (year days 40–80) does not produce as much carbon fixation according to this model.

Also plotted on the areal chlorophyll *a* and integral productivity time series are shipboard data collected near the mooring, at station S07 (16°N/62°E). (No productivity data are available from the mooring site.) Although we do not expect that these measures will closely agree with the model output, given spatial heterogeneity, the model value looks reasonable with respect to known carbon assimilation. Cruises

TN053 (November 1995) and TN054 (December 1995) occurred after the mooring was recovered; we chose to plot these for the previous year. With the exception of the eddy in December 1994, and to the extent that the model is correct, the values seem typical for the fall months. The chlorophyll *a* observed at the mooring is also consistent with shipboard data, showing the increase in values for each monsoon period. The comparison between shipboard and moored observations is discussed below.

4. Discussion

4.1. Verification of equations

Fig. 3 shows a comparison between vertical profiles of chlorophyll *a*, E_{PAR} and carbon assimilation as a means to evaluate the model in terms of shipboard data. In Fig. 3a, we compare chlorophyll *a* profiles from Station S07 on cruises TN043, TN045, TN049 and TN050, with comparable data generated by the mooring and the gridding scheme used to produce the chlorophyll *a* time series. The resulting $E_{PAR}(z)$ profiles using Eq. (4) and shipboard measured profiles are compared in Fig. 3b. Finally, in Fig. 3c, $P(z)$ is compared with measured in situ determinations of carbon assimilation.

Given spatial variability and incomplete data, the calculations we have made represent adequate approximations; exactly reproducing actual data from the moored sensors is a difficult task. The mooring chlorophyll *a* data overestimate shipboard values near the surface on two of the cruises. There are disagreements deeper in the water column, for example, the interpolation scheme records a deep chlorophyll *a* maximum during TN049 compared to that measured from shipboard sampling. However, the deeper chlorophyll *a* maxima do not contribute much carbon assimilation. The $E_{PAR}(z)$ model results are reasonably good approximations to the actual irradiance profiles found from the in situ PAR data loggers used in the in situ productivity experiments (Fig. 3b). Finally, carbon assimilation data measured on TN043 (23 January 1995), TN045 (30 March 1995), TN049 (3 August 1995), and TN050 (4 September 1995) at station S07 are compared to model results. As a function of depth, the model is a reasonable description of primary production; generally the agreement is better in the lower half of the euphotic zone than near the surface (Fig. 3c).

4.2. Phytoplankton absorption and quantum efficiency

Justification is required for our choice to keep the chlorophyll *a*-specific absorption coefficient used for the production calculation, $\bar{a}^*_{ps}$, constant. Bricaud et al. (1995) summarize a variety of data, and show that $\bar{a}^*_{ph}$, in general, increases with declining chlorophyll *a* values. The data show considerable variability, and thus a predictive relationship based on these data is not possible. In any case, Bricaud et al. (1995) suggest that the increase in $\bar{a}^*_{ph}$ with clearer, low chlorophyll *a*, waters is from greater

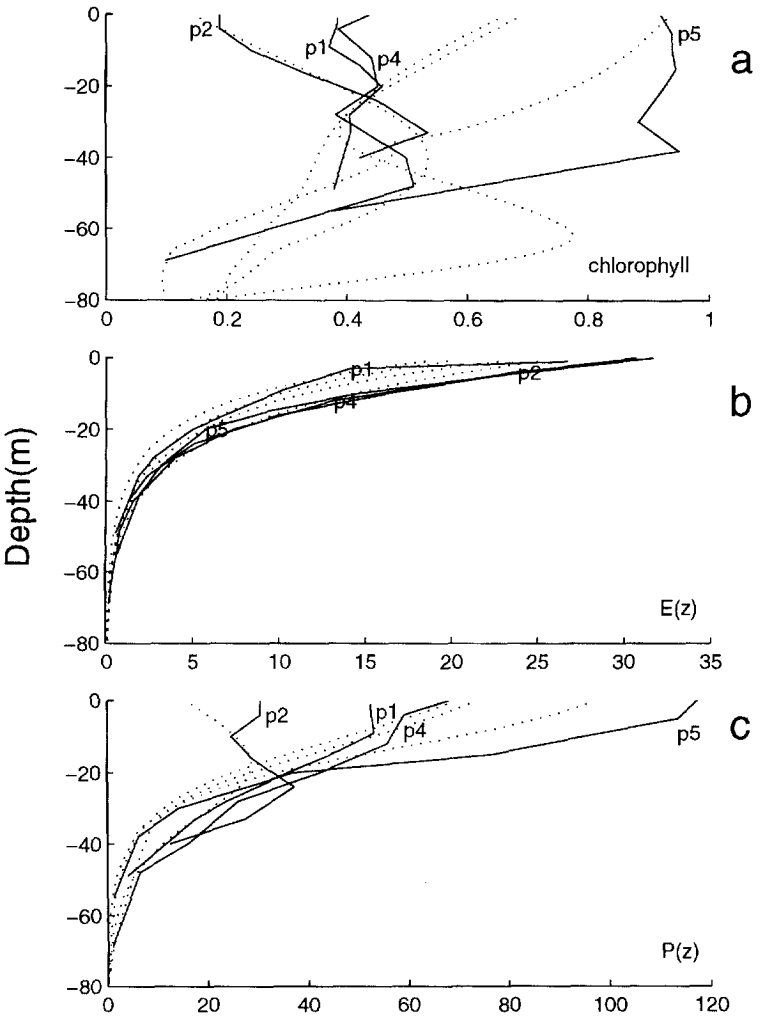

Fig. 3. Comparison of shipboard data from Station S07 (16°N, 62°E) with (a) the interpolated chlorophyll *a* values, (b) $E_{PAR}(z)$ (measured from shipboard), and carbon assimilation (c). p1 is cruise TN043 ("Process-1"), p2 is TN045 ("Process-2"), p4 is TN049 ("Process-4"), and p5 is TN050 ("Process5")

contribution by accessory pigments. The accessory pigments preferentially absorb in the blue, increasing the ratio of blue to red absorption. These pigments are also largely non-photosynthetic, also called photoprotectant because of their presumed role in dissipating excess radiant energy. These pigments are not directly related to carbon fixation. We have chosen, therefore, to keep $\bar{a}^*_{ph}$ (and $\bar{a}^*_{ps}$) constant, since any variation will be to protect the photosynthetic apparatus and not contribute to carbon assimilation. Similar findings were made by Sosik and Mitchell (1995) and Allali et al. (1997),

where they noted that absorption by photosynthetic pigments was less variable than total phytoplankton absorption.

The so-called "pigment package" effect (see Kirk, 1994) is also a source of variability in $\bar{a}^*_{ph}$. Bissett et al. (1997) conclude, however, that it is insignificant for their samples from the Arabian Sea. On the other hand, Allali et al. (1997) report significant package effect for their samples in the South Pacific. Although there is agreement on the lack of variability in the photosynthetic absorption, it is clear from the disagreements surrounding the package effect that we are not in a position to write a function for the seasonal variability in $\bar{a}^*_{ph}$ to use in our calculations.

Similar arguments can be made for quantum yield. Marra and Bidigare (1994) discuss the uncertainties in much of the previous field work. Typically, while ample evidence exists in the literature for variability, the causative factors are unclear (e.g., Schofield et al., 1993). The results of Babin et al. (1996) suggest a relationship between Φ_{max} and the combined concentration of nitrate and nitrite; however, in those data, phytoplankton absorption is equally important. We do not have the nutrient data at the same temporal resolution as the irradiance data to test the influence of nutrients as a factor in the variability of Φ_{max}.

4.3. Integral carbon assimilation and chlorophyll a as a function of season

Our estimate of primary production is dependent on a number of values, which, when reasonably chosen, approximate the level of in situ carbon assimilation observed from the ship (Figs. 2d and 3c). The advantage of the moored estimates is that, within the bounds by which we know the assigned values, we can examine variability in primary production over the season with a temporal resolution not otherwise possible. One way to analyze the meaning of the variability in integral primary production is to plot it as a function of areal chlorophyll *a*. On such a plot, primary production increases (along the *y*-axis) should always be accompanied by proportional increases in chlorophyll *a*. However, carbon assimilation lower than the optimal (below this "line") can occur because of lower photosynthetic efficiencies, or because $E_{PAR}(0^-)$ is reduced. In this portion of the plot, chlorophyll *a* also can change without corresponding changes to primary production, for example from grazing or sedimentation losses. Thus, only the right diagonal half of the plot (Fig. 4) can be occupied by data, with the maximum in chlorophyll *a*-specific primary production represented by a proportionality line. Our model uses a constant phytoplankton absorption and a singular relationship for the function describing the irradiance dependence of the quantum yield. Therefore, the only means by which integral production will vary is through changes in the irradiance supplied, the quantity of chlorophyll *a*, or in the water column distribution of chlorophyll *a* and its effect on $k_{tot}(z)$.

Early in the mooring time series, from October through December 1994, integral production increases in direct proportion to areal chlorophyll *a*, with the high values in each during this period being from an eddy that passed through the mooring site in early December (Sigurdson, 1996; Dickey et al., 1998, Fischer, 1997). In January, however, the primary production values fall below these, and this we attribute to the

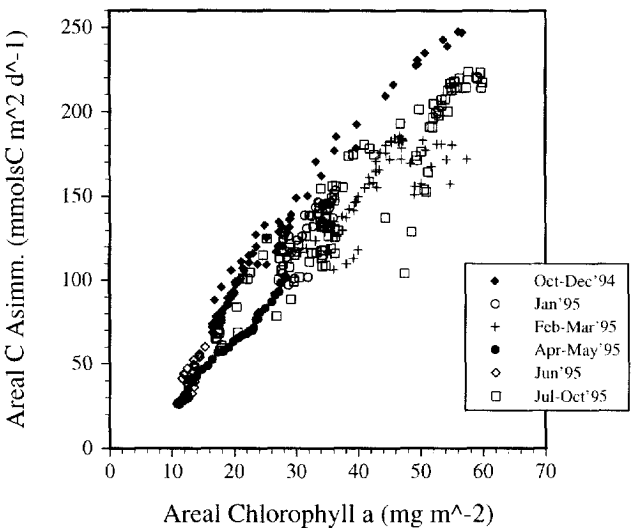

Fig. 4. Areal carbon assimilation plotted against areal chlorophyll *a*. Carbon assimilation was integrated over the euphotic zone, while chlorophyll *a* was integrated over the euphotic zone (when the euphotic zone was shallower than the mixed layer), or the mixed layer (when the mixed layer was deeper than the euphotic zone).

deeper mixed layers observed during this period. Deeper mixing may lead to greater irradiance limitation and mixing losses of chlorophyll *a* (Ho and Marra, 1994).

The increase in chlorophyll *a* seen in February does not exhibit the same rate of carbon assimilation conditions observed in the fall. One possibility is that the populations that grow upon re-stratification of the water column after the NE monsoon have characteristically lower rates of chlorophyll *a*-specific production than the previous populations. The RV *Thomas Thompson* did not visit the mooring site on TN045 until the end of March, about two weeks after the areal chlorophyll *a* maximum at the mooring (see Fig. 2d). On the northern line, however, a maximum in chlorophyll *a* was observed, and *Phaeocystis* was resident among the phytoplankton. Since there was no residual signal of a previous bloom of diatoms by the time *Thompson* reached station S07 and the mooring site, such as a high NO_3/SiO_4 ratio (Morrison et al., 1998), it is possible that the increase observed is the same as that observed two weeks earlier on the northern line, that is, a phytoplankton community dominated by *Phaeocystis*. Other than the negative evidence for diatoms, and the fact that *Phaeocystis* is a bloom-forming organism, we have little information in support of this supposition.

By April and May, the water column remains stratified, chlorophyll *a* declines, and integral production declines more rapidly, indicating that this might be a period of nutrient limitation. In June, the SW Monsoon begins. Chlorophyll *a* levels are low, but the values fall on the same line as in the previous fall. The deep mixed layers and lower incident irradiance probably prevent much accumulation of chlorophyll *a*;

however, increases are apparent in late July and August. The situation here is more complicated than in the first part of the record. There are rapid and large changes in carbon assimilation occurring at more or less constant areal quantities of chlorophyll *a*. There are also short periods of chlorophyll *a* loss with little change in integral carbon assimilation.

4.4. Grazing release vs the mixed layer depth

Although the data indicate periods of chlorophyll *a* loss while maintaining a relatively constant rate of carbon assimilation, the major change over the annual cycle at the mooring site is caused by changes in the mixed layer depth. Thus, the idea that phytoplankton biomass is controlled by irradiance availability and nutrients is consistent with the data that we present, at least for the most part. Inshore of Station S07 (the JGOFS station nearest the mooring), Smith et al. (1998) argue that the increase in phytoplankton associated with the SW Monsoon results from a decline in grazing pressure, when a major consumer, *Calanoides carnatus*, completes its life cycle in the surface layer and goes into diapause at depth. The loss of grazing pressure allows the phytoplankton bloom to materialize in July and August. Alternatively, the model of McCreary et al. (1996) suggests that for the central Arabian Sea the more important effect is the mixed layer depth, where stratification of the water column allows biomass to accumulate. It is possible, of course, that both factors are important, especially since the evidence for grazing release is for areas shoreward of the Findlater Jet, the location of the mooring. However, the biomass distribution that we observe is more consistent with the change in water column stratification. Biomass is diluted (and perhaps slowing production rates) during deepening periods of high wind stress, and allowing biomass to accumulate during more quiescent periods immediately following the monsoons.

Acknowledgements

This research was supported by ONR grants N00014-94-1-0450 (JM), N00014-96-1-0505 (TD), N00014-94-1-0161 (RAW), and NSF grant OCE-93-12355 (RTB). We thank M. Maccio, D. Manov, M. Stern, R. Trask, W. Ostrom, for assistance at sea, and S.L. Smith for continued encouragement.

References

Allali, K., Bricaud, A., Claustre, H., 1997. Spatial variations in the chlorophyll-specific absorption coefficients of phytoplankton and photosynthetically active pigments in the equatorial Pacific. Journal Geophysical Research, 102, 12,413–12,423.

Baker, K.S., Frouin, R., 1987. Relation between photosynthetically available radiation and total insolation at the ocean surface under clear skies. Limnology and Oceanography 32, 1370–1377.

Baumgartner, M., Brink, N.J. Ostrom, W.M., Trask, R.P., Weller, R.A., Dickey, T.D., Marra, J., 1997. Arabian Sea mixed layer dynamics experiment data report. WHOI Technical Report WHOI-97–08, p. 157.

Bidigare, R.R., Prezelin, B.B., Smith, R.C., 1992. Bio-optical models and the problems of scaling. In: Falkowski, P.G., Woodhead, A.V., Eds. Primary Production and Biogeochemical Cycling in the Sea, Plenum Press, New York pp. 175–212.

Bidigare, R.R., Smith, R.C., Baker, K.S., Marra, J., 1987. Optical characterization of primary production in the Sargasso Sea. Global Biogeochemical Cycles 1, 171–186.

Bricaud, A., Babin, M., Morel, A., Claustre, H., 1995. Variability in the chlorophyll-specific absorption coefficients of natural phytoplankton: analysis and parameterization. Journal Geophysical Research 100, 13,321–13,332.

Coble, P.G., Del Castillo, C., Avril, B., 1997. Distribution and optical properties of DOM in the Arabian Sea during the 1995 summer monsoon. Deep-Sea Research II 45, 2193–2223.

Dickey, T., Marra, J., Granata, T., Langdon, C., Hamilton, M., Wiggert, J., Siegel, D., Bratkovich, A., 1991. Concurrent high resolution bio-optical and physical time series observation in the Sargasso Sea during spring of 1987. Journal of Geophysical Research 95, 8643–8663.

Dickey, T., Granata, T., Marra, J., Langdon, C., Wiggert, J., Chai-Jochner, Z., Hamilton, M., Vasquez, J., Stramska, M., Bidigare, R., Siegel, D., 1993. Seasonal variability of bio-optical properties in the Sargasso Sea. Journal of Geophysical Research 98, 865–898.

Eriksen, C., Dahlen, J.M., Shillingford, J.T., 1982. An upper ocean moored current and density profiler applied to winter conditions near Bermuda. Journal of Geophysical Research 87, 7879–7902.

Fischer, A.S., 1997. Arabian Sea mixed layer deepening during the monsoon: observations and dynamics. M.S. Thesis, M.I.T. and W.H.O.I., Woods Hole, MA, 02543, 64 pp.

Ho, C., Kinkade, C.S., Langdon, C., Maccio, M., Marra, J., 1996. The forced upper ocean dynamics experiment in the Arabian Sea. Results from the multi-variable moored sensors from deployment-1 of the WHOI mooring., LDEO Technical Report LDEO-96-5, p. 19 + Figs., app.

Ho, C., Kinkade, C.S.,Langdon, C., Maccio, M., Marra, J., 1997. The forced upper ocean dynamics experiment in the Arabian Sea. Results from the multi-variable moored sensors from deployment-2 of the WHOI mooring. LDEO Technical Report LDEO-96-8, p. 19 + Figs., app.

Ho, C., Marra, J., 1994. Early-spring export of phytoplankton production in the Northeast Atlantic Ocean. Marine Ecology Progress Series 114, 197–202.

Kinkade, C.S., Marra, J., Dickey, T.D., Langdon, C., Sigurdson, D.E., Weller, R.A., 1998. Diel bio-optical variability in the Arabian Sea as observed from moored sensors. (In preparation).

Kirk, J.T.O., 1994. Light and Photosynthesis in Aquatic Systems, 2nd, ed. Cambridge Univ. Press, Cambridge.

Marra, J., 1995. Primary production in the North Atlantic Ocean: Scaling, measurements, and optical determinants. Philosophical Transactions of the Royal Society, London B 348, 153–160.

Marra, J., 1997. Analysis of diel variability in chlorophyll fluorescence. Journal of Marine Research 55, 767–784.

Marra, J., Dickey, T., Chamberlin, W.S., Ho, C. Granata, T., Kiefer, D.A., Langdon, C., Smith, R. Baker, K., Bidigare, R., Hamilton, M., 1992. The estimation of seasonal primary production from moored optical sensors in the Sargasso Sea. Journal of Geophysical Research, 97, 7399–7412.

McCreary, J.P., Jr. Kohler, K.E., Hood, R.R., Olson, D.B., 1996. A four-component model of biological activity in the Arabian Sea. Progress in Oceanography 37, 193–240.

Morrison, J., Codispoti, L., Gaurin, S., 1998. Seasonal variations of hydrographic and nutrient fields during the US JGOFS Arabian Sea Process Study. Deep-Sea Research II 45, 2053–2101.

Platt, T., Lewis, M., Geider, R., 1984. Thermodynamics of the pelagic ecosystem: elementary closure conditions for biological production in the open ocean. In: Fasham, M.J.R. (Ed.), Flows of Energy and Materials in Marine Ecosystems: Theory and Practice. Plenum Press, New York, pp. 49–84.

Rudnick, D., Weller, R.A., Eriksen, C., Dickey, T.D., Marra, J., Langdon, C., 1997. One-year moored observations of the Arabian Sea Monsoons. EOS, Transactions of the American Geophysical Union 78, 117,120–121.

Schofield, O., Prezelin, B.B., Bidigare, R.R., Smith, R.C., 1993. In situ photosynthetic yield. Correspondence to hydrographic and optical variability with the Southern California Bight. Marine Ecology Progress Series 93, 25–37.

Siegel, D.A., Dickey, T.D., 1987. On the parameterization of irradiance for open ocean photoprocesses. Journal of Geophysical Research 92, 14,648–14,662.

Sigurdson, D., 1996. Analysis of physical and bio-optical variability in the Arabian Sea during the northeast monsoon of 1994. M.S. Thesis, Univ. So. California, 124pp.

Sigurdson, D., Dickey, T.D., Manov, D. 1995. Arabian Sea mooring data report. Deployment #1, 15 October, 1994–20 April, 1995. Ocean Physics Laboratory Technical Report #OPL-2-95, 26pp.

Sigurdson, D., Dickey, T.D., Manov, D. 1996. Arabian Sea mooring data report. Deployment #2, April 22 – October 15, 1995. Ocean Physics Laboratory Tech. Rep. #OPL-2–96, 26pp.

Smith, R.C., Marra, J., Perry, M. J., Swift, E., Baker, K. S., Buskey, E., Kiefer, D.A., 1988. Estimation of photon budget for the upper ocean in the Sargasso Sea. Limnology and Oceanography 34, 1673–1693.

Smith, S.L., 1997. The U.S. JGOFS Arabian Sea Expedition. Deep-Sea Research II, this issue

Smith, S.L., Roman, M., Wishner, K., Gowing, M., Codispoti, L., Barber, R.T., Marra, J., Prusova, I., Flagg, C., 1998. Seasonal response of mesozooplankton to monsoonal reversals in the Arabian Sea. Deep-Sea Research II 45, 2367–2403.

Sosik, H.M., Mitchell, B.G., 1995. Light absorption by phytoplankton, photosynthetic pigments and detritus in the California Current System. Deep-Sea Research 42, 1717–1748.

Stramska, M., Dickey, T.D., 1992. Variability of bio-optical properties of the upper ocean associated with diel cycles in phytoplankton population. Journal of Geophysical Research 97, 17,873–17,887.

Trask, R., Weller, R.A., Ostrom, W.M., 1995a. Arabian Sea mixed layer dynamics experiment. Mooring deployment cruise report, R/V Thomas Thompson Cruise No. 40, 11–25 October 1994. WHOI Technical Report WHOI-95–01.

Trask, R., Weller, R.A., Ostrom, W.M., 1995b. Arabian Sea mixed layer dynamics experiment. Mooring deployment cruise report, R/V Thomas Thompson Cruise No. 46, 14–29 April, 1995. WHOI Technical Report WHOI-95–14.

Weller, R.A., Baumgartner, M.F., Josey, S.A., Fischer, A.S., Kindle, J., 1998. Atmospheric forcing in the Arabian Sea during 1994–1995: observations and comparisons with climatology and models. Deep-Sea Research II 45, 1961–1997.

Wessel, P., Smith, W.H.F., 1992. Free software helps map and display data. EOS, Transactions of the American Geophysical Union, 72, 445–446,.

Wozniak, B., Dera, J., Koblentz-Mishke, O., 1992. Modeling the relationship between primary production, optical properties and nutrients in the sea (as a basis for indirectly estimating primary production). Proceedings of SPIE, Ocean Optics XI, vol. 1750, pp. 246–275.

Zaneveld, J.R.Z., Kitchen, J.C., Mueller, J.L., 1993. Vertical structure of productivity and its vertical integration as derived from remotely sensed observations. Limnology and Oceanography 38, 1384–1402.